Journal of Clinical and Nursing Research, 2025, Volume 9, Issue 12
http://ojs.bbwpublisher.com/index.php/JCNR
Online ISSN: 2208-3693
Print ISSN: 2208-3685

The Predictive Value of Combined Synthetic MRI Features and PSAD for Clinically Significant Prostate Cancer

Yunqi Yang, Yukang Hu, Chunhua Xia*

The Third Affiliated Hospital of Anhui Medical University (Hefei First People's Hospital), Hefei 230000, Anhui, China

**Corresponding author: Chunhua Xia, xiachunhua3775@sina.com*

Abstract: *Objective*: To investigate the diagnostic and predictive value of MRI features combined with clinical indicators for prostate cancer (PCa) and clinically significant prostate cancer (csPCa), and to establish a non-invasive combined model. *Methods*: A total of 36 patients with pathologically confirmed benign lesions (44 foci) and 23 patients with PCa (49 foci), including 25 foci of csPCa and 68 foci of non-csPCa, were included. SyMRI quantitative maps and clinical indicators were collected, and 224 imaging features were extracted. The intra- and inter-group correlation coefficients (ICC) for each feature were calculated using intra- and inter-group correlation analysis, and features with an ICC > 0.75 were selected as stable features that could be reproducibly extracted. Independent predictors were screened using logistic regression to construct single and combined models, and the performance was evaluated using ROC curves. *Results*: Age, PSAD, PD map contrast, and T2 map joint entropy were significantly higher in the PCa group compared to the benign group, while the median ADC was significantly lower ($p < 0.05$). The above-mentioned indicators were significantly correlated with PCa and csPCa, and the diagnostic performance of the combined model was superior to that of a single MRI or clinical model. *Conclusion*: MRI features combined with PSAD can effectively differentiate PCa and predict csPCa, providing a non-invasive quantitative diagnostic basis for clinical practice.

Keywords: Prostate cancer; Prostate-specific antigen; Synthetic magnetic resonance imaging; Predictive value

Online publication: Dec 31, 2025

1. Introduction

Prostate cancer (PCa) is the second most common type of cancer among men worldwide. In 2020, over 1.4 million new cases of prostate cancer were reported, and it remains the fifth leading cause of cancer-related deaths in men [1]. The monitoring and treatment approaches for PCa are closely related to the Gleason Grade Group (GG) classification. Clinically, prostate-specific antigen (PSA) screening has traditionally been used for prostate cancer

detection [2]. Guidelines recommend PSA-based prostate cancer screening for men aged 50 and above, or those aged 45 and above with a family history of prostate cancer, after fully informing them of the screening risks [3]. PSA is a glycoprotein expressed by prostate tissue. However, due to the relatively low sensitivity and specificity of PSA in detecting early-stage prostate cancer, pathology remains the gold standard for diagnosing PCa. To reduce unnecessary biopsies and overtreatment of low-grade prostate cancer, there is an urgent need for a non-invasive, rapid diagnostic approach.

Clinically, prostate cancer (PCa) with a Gleason Score (GS) of ≥ 3 + 4, a tumor volume of ≥ 0.5 cm^3, or extracapsular extension is defined as clinically significant prostate cancer (csPCa) [4]. csPCa is an aggressive and highly malignant tumor that requires a combination of multiple treatment modalities in clinical practice to improve patient survival rates. In contrast, clinically insignificant prostate cancer (CIPC), due to its slow growth rate and low malignancy, is recommended for active surveillance without the need for treatment in clinical settings [5]. Early and accurate diagnosis of csPCa holds significant guiding importance for formulating treatment plans and predicting patient outcomes.

The Prostate Imaging Reporting and Data System (PI-RADS) is a standardized system for prostate MRI imaging and interpretation [6,7]. However, the evaluation methods in PI-RADS are predominantly subjective, lacking objective quantitative indicators, and suffer from issues such as low positive predictive value, high false-positive rates, and poor reproducibility. Currently, the commonly used T1 mapping and T2 mapping sequence scans are time-consuming and prone to patient movement issues, making it difficult to promote their clinical application [8].

In recent years, synthetic magnetic resonance imaging (synthetic MRI, SyMRI) technology has been introduced and applied in clinical settings. This technique enables the acquisition of multiple contrast images, such as T1 and T2, as well as absolute quantitative maps, through a single scan. Furthermore, the quantitative maps generated by this technology demonstrate good consistency with conventional quantitative relaxation techniques [8]. Arita et al. also found that for clinically significant cancer and PI-RADS category 3 lesions, there were no significant differences in diagnostic performance between synthetic MRI and both biparametric MRI (bpMRI) and dynamic contrast-enhanced MRI (DCE-MRI) ($p = 0.11–0.79$) [9]. Texture analysis involves studying the local characteristics, patterns of change, and distribution modes of pixel gray-level values by analyzing the grayscale information in digital images, thereby quantifying the heterogeneity of lesions. Using SyMRI quantitative maps for texture analysis holds promise in addressing the issue of weak reproducibility among different researchers and contributes to establishing diagnostic criteria for quantitatively predicting clinically significant prostate cancer (csPCa). This study aims to explore the diagnostic and predictive value of synthetic MRI texture features combined with PSA-related indicators, such as prostate-specific antigen density (PSAD), for prostate cancer and csPCa. The goal is to establish a non-invasive, quantitative combined predictive model that provides a more accurate basis for clinical diagnosis and treatment.

2. Materials and methods

2.1. General information

This study was approved by the Ethics Committee of the Third Affiliated Hospital of Anhui Medical University (Hefei First People's Hospital). Case data of patients who underwent prostate MRI examinations and obtained pathological results via surgery or biopsy from April 2024 to October 2025 were collected. The inclusion and exclusion criteria were as follows: corresponding pathological results were obtained after the MRI examination with an interval of no more than 3 months; all patients had preoperative serum PSA levels; none of them had

received radiotherapy, chemotherapy, endocrine therapy, or other relevant treatments prior to the MRI examination, nor had they undergone prostate biopsy within 6 weeks.

2.2. Instruments and methods

A GE SIGNA Architect 3.0 T magnetic resonance scanner was used, equipped with a 28-channel phased-array abdominal coil. The scanning sequences included axial, coronal, and sagittal T2-weighted imaging, axial T1-weighted imaging, axial DWI with b-values of 50 and 1400 s/mm^2, and axial SyMRI. SyMRI utilized a multi-dynamic multi-echo (MDME) sequence for imaging, which consisted of 2 echo times and 4 delay times, generating a total of 8 raw images. The scanning parameters are detailed in the following table. ADC maps were automatically generated from the DWI images on the scanner console. Post-processing of the MDME raw images was performed using software to generate quantitative maps of T1, T2, and PD (refer **Table 1**).

Table 1. The detailed acquisition parameters of the MRI sequences.

Parameters	T1WI	T2WI	DWI	Synthetic MRI
Sequence	Fast spin echo	Fast spin echo	spin-echo echo-planar	QRAPMASTER
Imaging plane	Axial	Axial, coronal, sagittal	Axial	Axial
Repetition time (msec)	7	4100,4200,5700	6400	4000
Eeho time (msec)	7	88,92,102	80	14/92
Inversion time (msec)	-	-	120	170/670/1840/3840
Flip angle (degrees)	111	111,110,110	90	90
Slice thickness/gap (mm)	4/1	4/1,4/1,4/1	4/1	4/1
Field of view (mm)	300 × 300	240 × 240,280 × 280,240 × 240	240 × 240	300 × 300
Matrix (frequency × phase)	320 × 256	320 × 256,352 × 352,320 × 256	96 × 128	320 × 256
Number of excitation	1	2, 2, 2	12	1
Echo train length	4	20,18,30	-	16
Bandwidth (kHz)	83.33	83.33,41.67,62.5	250	50
b values (s/mm^2)	-	-	50/1400	-
Acceleration factor	2	2	2	2
Acquisition time (min: s)	01:39	02:05,02:15,01:57	04:10	04:32

T1WI: T1 weighted imaging; T2WI: T2 weighted imaging; DWI: diffusion weighted imaging; MRI: magnetic resonance imaging; QRAPMASTER: quantification of relaxation times and proton density by multi-echo acquisition of a saturation-recovery using turbo spin-echo readout

2.3. Image analysis

Post-process the raw images scanned by the SyMRI sequence on the host computer to generate quantitative maps of Tl, T2, and PD. Based on the puncture site, manually delineate the region of interest (ROI) on the SyMRI quantitative images using ITK-SNAP software, and then register the SyMRI and DWI images. Copy the ROI to the registered DWI and ADC maps. Texture features are extracted from histograms, shape features, and gray-level co-occurrence matrices (GLCM), with a total of 224 features extracted.

2.4. Statistical method design

Statistical analysis is conducted using IBM SPSS 26.0 software. Measurement data are first evaluated for normality distribution using the Kolmogorov–Smirnov test: data conforming to a normal distribution are expressed as "mean ± standard deviation", and comparisons between groups are made using the independent samples *t*-test; data not conforming to a normal distribution are expressed as "median (interquartile range)", and comparisons between groups are made using the Mann Whitney U test. Compare the characteristic differences between benign and malignant prostate lesions, as well as between csPCa and non-csPCa (including imaging features such as T1map_mean and T2map_mean, as well as clinical indicators such as age and PSAD).

Logistic regression analysis was employed, with the aforementioned 230 features (224 imaging features and 6 clinical indicators) serving as independent variables, and "whether it is prostate cancer" or "whether it is csPCa" acting as the dependent variables. Variables significantly correlated with the dependent variables were screened out, and independent predictors with statistical significance were retained. Based on the above analysis results, a combined predictive model integrating "MR features + clinical indicators" was constructed, alongside single MR feature and single clinical indicator models for comparison. Receiver Operating Characteristic (ROC) curve analysis was used to evaluate the diagnostic performance of each model, calculating the Area Under the Curve (AUC), 95% Confidence Interval (CI), sensitivity, specificity, and optimal diagnostic threshold. The DeLong test was utilized to compare differences in AUC among different models, with $p < 0.05$ indicating statistical significance.

3. Results

A total of 36 benign patients and 23 prostate cancer patients were ultimately included. Counting by lesions, there were 44 lesions in the benign prostate lesion group and 49 in the malignant group; based on whether it was csPCa, they were further divided into 25 lesions in the csPCa group and 68 in the non-csPCa group. All included cases were pathologically confirmed. The mean age was 68.52 ± 6.31 years in the benign group and 73.89 ± 8.15 years in the prostate cancer group, with a significant increase in age observed in the prostate cancer group. In addition, PSAD, PDmap_original_glcm_Contrast, and T2map_original_glcm_JointEntropy in the prostate cancer group were also significantly higher than those in the benign group, while ADC_original_firstorder_Median showed a significant decrease (**Table 2**).

Table 2. Comparison of baseline data between the two groups of patients

Variable	Benign group (n = 44)	Prostate cancer (n = 49)	*p*-value
Age (years)	68.52 ± 6.31	73.89 ± 8.15	0.021
PSAD (ng/mL^2)	0.18 ± 0.07	0.39 ± 0.15	< 0.001
ADC_original_firstorder_Median (×10^{-3} mm^2/s)	1.42 ± 0.23	0.98 ± 0.19	< 0.001
PDmap_original_glcm_Contrast	12.35 ± 4.12	18.67 ± 5.83	0.003
T2map_original_glcm_JointEntropy	2.15 ± 0.68	3.42 ± 0.95	< 0.001

Among the 224 extracted imaging features, logistic regression analysis revealed that ADC_original_firstorder_Median exhibited an inverse trend with the occurrence of PCA. A decrease in its value suggested restricted diffusion of water molecules, consistent with the pathological characteristic of increased cellular density in cancerous lesions. Conversely, PSAD, PDmap_original_glcm_Contrast, and T2map_original_glcm_JointEntropy were

positively correlated with the occurrence of PCA. For clinically significant prostate cancer, we similarly found that Age, PDmap_original_glcm_Contrast, and T2map_original_glcm_JointEntropy were positively correlated with its occurrence, while ADC_original_firstorder_Median demonstrated an inverse trend (**Table 3**). This study has evaluated the predictive capabilities of these indicators using ROC curves and found that the predictive power of a single MRI indicator or clinical indicator was lower than that of the combined MRI model, and even lower than the combination of clinical and MRI indicators. This trend was consistent in diagnosing benign conditions versus PCA and determining whether the prostate cancer was clinically significant (**Figure 1**).

Table 3. Association analysis of key indicators with clinical subtypes

Group	Variables	OR	95%CI	p
Benign vs malignant differentiation	PSAD	1.46	1.00–1.74	0.041
	ADC_original_firstorder_Median	0.0008	0.00–0.39	0.037
	PDmap_original_glcm_Contrast	1.04	1.02–1.07	0.004
	T2map_original_glcm_JointEntropy	6.52	1.16–52.58	0.049
Clinical vs non-clinical subtype differentiation	Age	1.18	1.04–1.39	0.016
	ADC_original_firstorder_Median	2.09 × 10-6	0.00–0.01	0.005
	PDmap_original_glcm_Contrast	1.05	1.02–1.10	0.006
	T2map_original_glcm_JointEntropy	1573.3	23.06–2006221.70	0.008

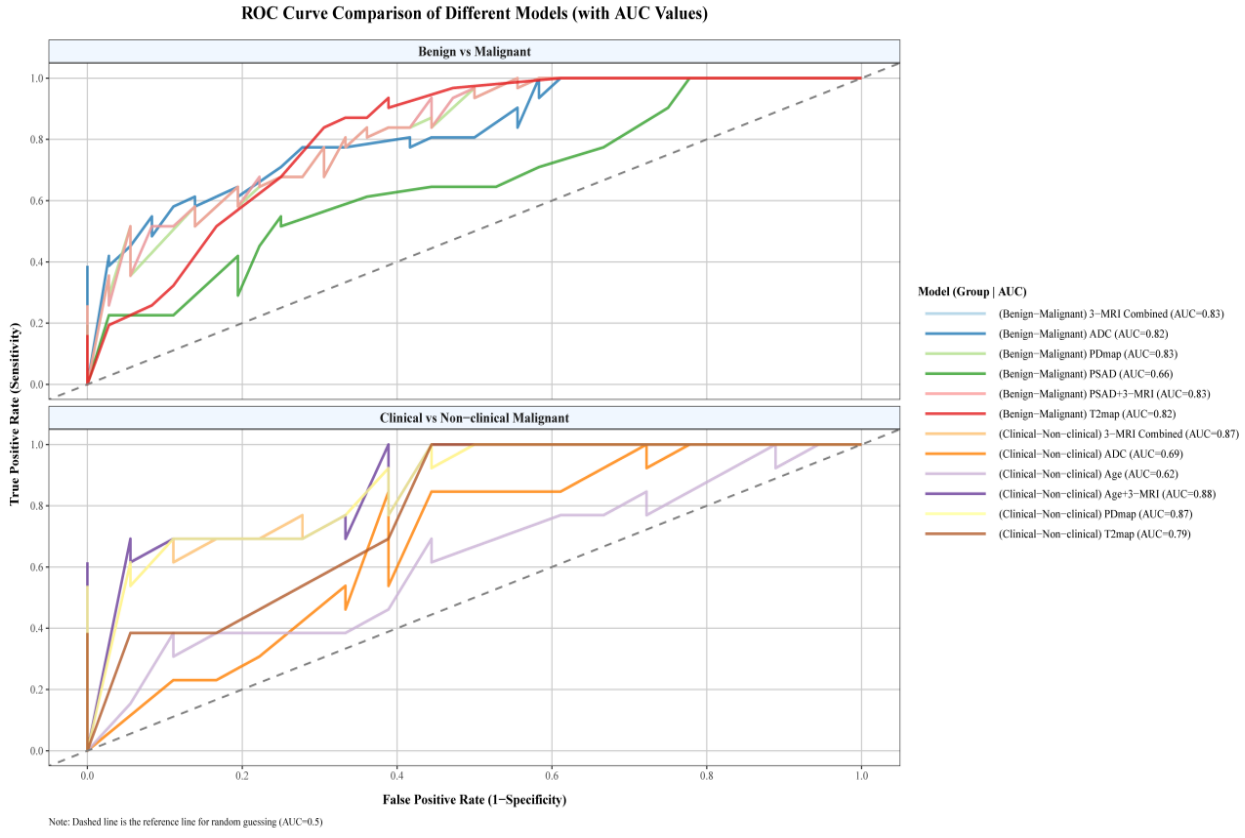

Figure 1. ROC curve comparison of different model (with AUC values).

4. Discussion

Prostate cancer is one of the most common malignant tumors in the male urinary system, with its epidemiology exhibiting significant characteristics of "age dependency" and "regional heterogeneity" [10]. Globally, prostate cancer ranks second in incidence among male malignant tumors and rises exponentially with age, with a notable increase in incidence among men over 60 years old, reaching its peak in the 70–80 age group [11]. The stratification of clinical significance in prostate cancer is one of the core focuses of current diagnostic and treatment decision-making, given its distinct epidemiological characteristics and biological behaviors. Clinically significant prostate cancer (CSPC) typically refers to cancerous lesions with a risk of clinical progression (such as a Gleason score ≥ 7, large tumor volume, or capsular invasion), whereas non-clinically significant prostate cancer (non-CSPC) often presents as indolent lesions. These two types of prostate cancer differ fundamentally in terms of diagnostic and treatment strategies as well as prognosis [12,13]. This study included 36 patients with pathologically confirmed benign prostatic lesions and 23 patients with prostate cancer. In terms of lesion distribution, benign lesions predominantly occurred in the transition zone, while malignant lesions were more common in the peripheral zone. This finding aligns perfectly with the epidemiological characteristic of prostate cancer being "predominantly peripheral zone-originating" and the pathological distribution characteristic of benign hyperplasia being "primarily transition zone-based", providing a pathological basis for the rationality of lesion localization in subsequent radiomics analysis [14–16]. From a clinical perspective, patients in the prostate cancer group were significantly older than those in the benign group, aligning with the epidemiological pattern of prostate cancer's "age dependency". As age increases, the risk of gene mutations in prostate epithelial cells accumulates, leading to a significantly higher likelihood of cancerous lesions. This further confirms the clinical significance of age as a risk factor for prostate cancer [17].

In terms of imaging and derived omics parameters, the prostate cancer group exhibited significantly higher values of PSAD, PDmap_original_glcm_Contrast, and T2map_original_glcm_JointEntropy compared to the benign group, while ADC_original_firstorder_Median was notably lower. Among these, the increase in PSAD reflects the heightened antigen secretion due to abnormal proliferation of cancer cells, serving as a crucial derived indicator for breaking through the PSA diagnostic gray zone. The decrease in ADC values is directly related to restricted water molecule diffusion caused by high cellular density and narrow extracellular spaces in cancerous lesions, providing a core quantitative basis for diagnosing prostate cancer using magnetic resonance diffusion-weighted imaging (DWI) [18]. The elevation in PDmap contrast and T2 map joint entropy essentially represents the microscopic structural characteristics of uneven cell proliferation within cancerous lesions, with a mixture of necrotic and proliferative areas, as reflected in the imaging texture features. This reveals the heterogeneity of tumor tissue from the perspective of texture omics. From the perspective of diagnostic performance, Receiver Operating Characteristic (ROC) curve analysis revealed that the model combining clinical indicators with multimodal MRI features had a significantly higher Area Under the Curve (AUC) compared to models based solely on a single MRI modality or purely clinical indicators. This result underscores the value of multidimensional integration of "clinical-radiomics", clinical indicators provide risk stratification at the population level, while MRI diffusion and texture features enable precise localization and characterization at the microstructural level of the lesion. The combination of these two approaches effectively compensates for the information limitations of single modalities, offering more comprehensive decision support for the "early identification and risk stratification" of prostate cancer [19].

5. Conclusion

In summary, through multidimensional analysis encompassing clinical, imaging, and radiomic data, this study not only validated the independent value of age, Prostate-Specific Antigen Density (PSAD), Apparent Diffusion Coefficient (ADC), and texture radiomic parameters in differentiating benign from malignant prostate lesions but also demonstrated, through a multi-model fusion strategy, the advantages of integrating "clinical-radiomics" for precise diagnosis of prostate cancer. This provides evidence-based support for optimizing the clinical diagnosis and treatment pathways for prostate cancer.

Disclosure statement

The authors declare no conflict of interest.

References

[1] Sung H, Ferlay J, Siegel R, et al., 2021, Global Cancer Statistics 2020: GLOBOCAN Estimates of Incidence and Mortality Worldwide for 36 Cancers in 185 Countries. CA Cancer J Clin, 71(3): 209–249.

[2] Adamaki M, Zoupourlis V, 2021, Prostate Cancer Biomarkers: From Diagnosis to Prognosis and Precision-Guided Therapeutics. Pharmacol Ther, 228: 107932.

[3] Williams I, McVey A, Perera S, et al., 2022, Modern Paradigms for Prostate Cancer Detection and Management. Med J Aust, 217(8): 424–433.

[4] Turkbey B, Rosenkrantz A, Haider M, et al., 2019, Prostate Imaging Reporting and Data System Version 2.1: 2019 Update of Prostate Imaging Reporting and Data System Version 2. Eur Urol, 76(3): 340–351.

[5] Meng T, Liu H, Zhang W, et al., 2020, Application of Integrated Magnetic Resonance Imaging Relaxation Time Quantification in the Diagnosis of Prostate Cancer. Journal of Clinical Radiology, 39(03): 605–608.

[6] Peng T, Xiao J, Li L, et al., 2021, Can the Analysis of Multiparameter MRI and Clinical Parameters Based on Machine Learning Enhance the Diagnostic Performance for Clinically Significant Prostate Cancer. Int J Comput Assist Radiol Surg, 16(12): 2235–2249.

[7] Urraro F, Nardone V, Reginelli A, et al., 2021, MRI Radiomics in Prostate Cancer: A Study on Reliability. Front Oncol, 11: 805137.

[8] Gao Z, Xu X, Sun H, et al., 2024, The Diagnostic and Assessment Value of Synthetic Magnetic Resonance Imaging in Determining the Aggressiveness of Prostate Cancer. Quant Imaging Med Surg, 14(8): 5473–5489.

[9] Arita Y, Akita H, Fujiwara H, et al., 2022, Synthetic Magnetic Resonance Imaging for Evaluating Primary Prostate Cancer: Diagnostic Potential of a Non-Contrast-Enhanced Bi-Parametric Approach Augmented with Relaxometry Measurements. Eur J Radiol Open, 9: 100403.

[10] Trecarten S, Sunnapwar A, Clarke G, et al., 2024, Prostate MRI for Identifying Clinically Significant Prostate Cancer: Updates and Future Prospects. Adv Cancer Res, 161: 71–118.

[11] Kurokawa G, Mori K, Sasaki H, et al., 2024, Efficacy of Magnetic Resonance Imaging/Ultrasound-Guided Targeted Biopsy in Detecting Clinically Significant Prostate Cancer. Anticancer Res, 44(02): 679–686.

[12] Kamecki H, Tokarczyk A, Dębowska M, et al., 2025, A Straightforward Nomogram for Predicting Clinically Significant Prostate Cancer During MRI-Guided Biopsy in Patients with Mild PSA Elevation and Normal DRE. Cancers, 17(05): 753.

[13] Wibmer A, Lefkowitz R, Lakhman Y, et al., 2022, The MRI-Detectability of Clinically Significant Prostate Cancer Is

Associated with Oncologic Outcomes After Prostatectomy. Clin Genitourin Cancer, 20(04): 319–325.

[14] Kilic M, Madendere S, Vural M, et al., 2023, The Significance of the Size and Number of Index Lesions in Diagnosing Clinically Significant Prostate Cancer in Patients with PI-RADS 4 Lesions Who Underwent In-Bore MRI-Guided Prostate Biopsy. World J Urol, 41(02): 449–454.

[15] Frisbie J, Van Besien A, Lee A, et al., 2022, PSA Density Complements the Prostate mpMRI PI-RADS Scoring System for Risk Stratification of Clinically Significant Prostate Cancer. Prostate Cancer Prostatic Dis, 26(02): 347–352.]

[16] Yamamoto T, Okada H, Matsunaga N, et al., 2024, Clinical Characteristics and Pathological Features of Undetectable Clinically Significant Prostate Cancer on Multiparametric Magnetic Resonance Imaging: A Single-Center Retrospective Study. J Clin Imaging Sci, 14: 20.

[17] Szempliński S, Kamecki H, Dębowska M, et al., 2022, Predictors of Clinically Significant Prostate Cancer in Patients with PI-RADS Categories 3–5 Undergoing Magnetic Resonance Imaging–Ultrasound Fusion Biopsy of the Prostate. J Clin Med, 12(01): 156.

[18] Tamada T, Takeuchi M, Watanabe H, et al., 2024, Differentiating Clinically Significant Prostate Cancer from Clinically Insignificant Prostate Cancer Using Qualitative and Semi-Quantitative Indices of Dynamic Contrast-Enhanced MRI. Discover Oncol, 15(01): 770.

[19] Hassanzadeh E, Alessandrino F, Olubiyi O, et al., 2018, Comparison of Quantitative Apparent Diffusion Coefficient Parameters with Prostate Imaging Reporting and Data System V2 Assessment for Detection of Clinically Significant Peripheral Zone Prostate Cancer. Abdom Radiol, 43(05): 1237–1244.